

Effects of mesoscale eddies on the flow of the Alaskan Stream

Wieslaw Maslowski,¹ Ricardo Roman,¹ and Jaclyn Clement Kinney¹

Received 15 May 2007; revised 27 January 2008; accepted 5 March 2008; published 24 July 2008.

[1] Using a high-resolution, pan-Arctic ice-ocean model forced with realistic atmospheric data, we examine the mean transport and temporal and spatial variability within the Alaskan Stream. Model results are analyzed and compared with observations, including satellite altimetry and CTD measurements. The mean net transport of the Alaskan Stream is found to be between 34 and 44 Sv, intensifying downstream. Mesoscale eddies are found to periodically move along the path of the Alaskan Stream and alter the mean position of the typically westward-flowing current. However, the strength of the current is not reduced as an anticyclonic eddy passes a point along the path. Instead, there appears to be an offshore (or southward) shift in the current velocity core. Stationary measurement instruments may not be able to detect this shift in position over the slope if their southernmost location does not coincide with the current shift due to an eddy. This may result in recording of a weakened or sometimes reversed flow. Finally, we examine and demonstrate that modeled eddies within the Alaskan Stream have dominant effect on northward transport and variability through the eastern and central Aleutian Island passes.

Citation: Maslowski, W., R. Roman, and J. C. Kinney (2008), Effects of mesoscale eddies on the flow of the Alaskan Stream, *J. Geophys. Res.*, 113, C07036, doi:10.1029/2007JC004341.

1. Introduction

[2] The Alaskan Stream is an intense, narrow (~50–80 km) and deep (>3000 m) current, which represents the northern boundary of the Pacific sub-Arctic gyre [Stabeno and Reed, 1992; Reed and Stabeno, 1999]. Flowing from east to west, the Alaskan Stream extends from the head of the Gulf of Alaska to the most western Aleutian Islands. In the mean state, the fast-moving current intensifies as it flows westward along the southern edge of the Aleutian Island Arc, reaching an estimated volume transport of 38.8 Sv near 180°W, based on a 6000 dbar reference level [Rodén, 1995; Chen and Firing, 2006]. The Alaskan Stream has a significant influence on the Bering Sea, as the primary source of warm and relatively fresh water for mass and property fluxes through the Aleutian passes, which contribute to the Aleutian North Slope Current and Bering Slope Current [Reed, 1990; Reed and Stabeno, 1999].

[3] Variability in the Alaskan Stream flow, as well as in the Aleutian Island throughflow, plays a key role in the delicate balance of both the water properties and the circulation within the Bering Sea [Okkonen *et al.*, 2003; Onishi and Ohtani, 1999; Reed and Stabeno, 1989; Rodén, 1995]. Major disturbances created by southward shifts in the Alaskan Stream and eddies propagating along the Aleutian Island Arc produce the largest deviations, which have been explored in several different studies. One of such studies concerning flow anomalies in the Alaskan Stream is presented by Reed and Stabeno [1989]. They observed,

through data gathered from current moorings located southwest of Kodiak Island, that the Alaskan Stream had periods of negligible westward flow, appearing nearly absent during spring of both 1986 and 1987. Monitoring the path of satellite-tracked buoys within this region, they concluded that the Alaskan Stream had not disappeared during these time periods, but rather underwent a seaward shift (south of the current mooring station) without experiencing a reduction in speed. Evidence of reductions in the volume transport of the Alaskan Stream is presented by Reed and Stabeno [1999]. CTD data gathered from stations located near 170°W measured unusually low westward flow during May 1997, while satellite altimetry data during the same period also revealed the presence of a strong anticyclonic eddy centered near 167°W. Also, Musgrave *et al.* [1992] mention frequent anticyclonic eddies present in both hydrographic data and the dynamic topography. Finally, eddies along the Alaskan Stream have been simulated in models [e.g., Cummins and Mysak, 1988]. However, all these studies present rather limited information about the effect of eddies. Their findings, though, indicate that the presence of eddy-like features along the Alaskan Stream complicate transport calculations due to increased variability and shifts in the location of the current.

[4] The Alaskan Stream, as evidenced by the above studies, is an intense boundary current with significant, semiperiodic fluctuations that can alter its course and speed; however, long-term data is needed to determine the development and life cycle of these meanders and eddies [Onishi and Ohtani, 1999]. In Crawford *et al.* [2000], 6 years of TOPEX/Poseidon (T/P) data measured the presence of six anticyclonic eddies in the Alaskan Stream during September 1992 through September 1998. The sea surface height anomalies and eddy diameter approached 72 cm and aver-

¹Department of Oceanography, Naval Postgraduate School, Monterey, California, USA.

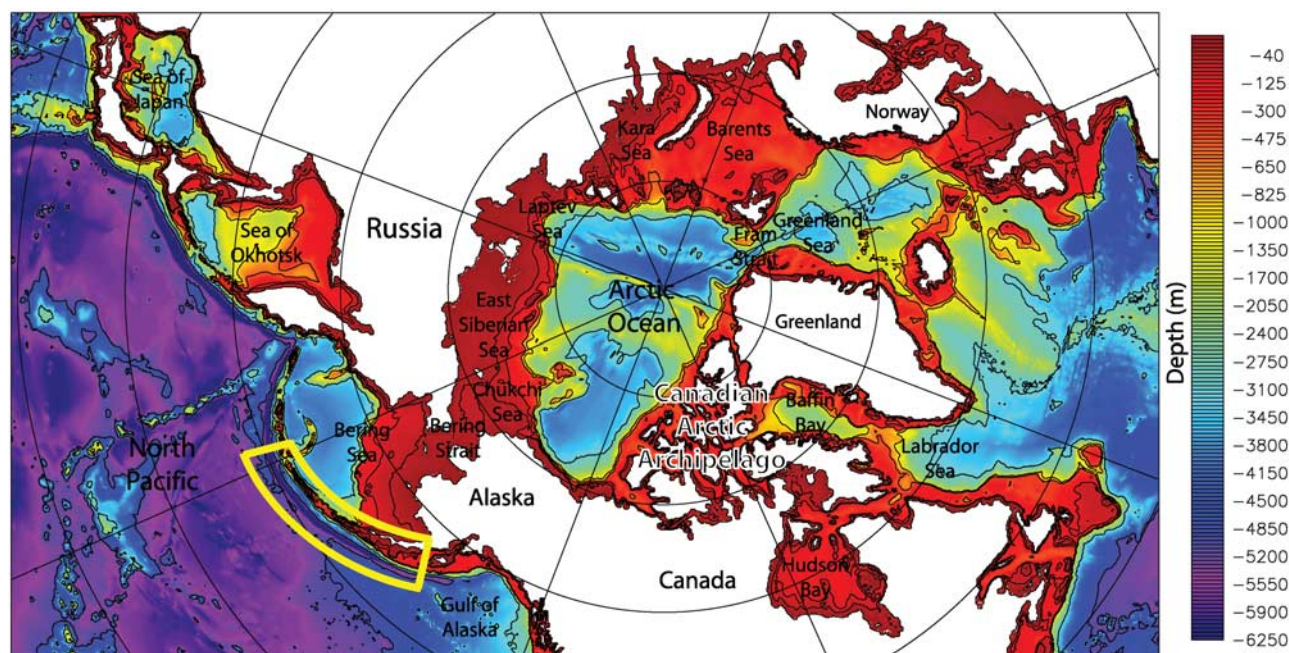


Figure 1. Model domain and bathymetry (m). The region of interest is outlined in yellow.

aged 160 km respectively, while the mean lifespan was 1 to 3 years. Of the six eddies, some formed near the Alaskan panhandle, while others began propagating just south of Shelikof Strait with an estimated phase speed of ~ 2.5 km day $^{-1}$. Because the Alaskan Stream represents the largest source of transport into the Bering Sea, these long-lived eddies may significantly alter both the physical and biological structure of the Bering Sea [Okkonen, 1992, 1996].

[5] The primary goal of this article is to analyze output from a numerical model to investigate the long-term effect of mesoscale eddies propagating along the Aleutian trench on the westward volume and property transport of the Alaskan Stream and on exchanges through selected Aleutian Island passes. Model results will be compared with observational data to include volume transport, water column velocities, and eddy propagation.

2. Model Description

[6] The coupled sea ice-ocean model has a horizontal grid spacing of $1/12^\circ$ (or ~ 9 km) and 45 vertical depth layers with eight levels in the upper 50 m. This horizontal grid permits proper representation of the circulation including mesoscale eddies of order hundreds km, commonly observed in the Gulf of Alaska [Okkonen, 1992; Meyers and Basu, 1999; Crawford *et al.*, 2000; Okkonen *et al.*, 2003; Crawford, 2005; Ladd *et al.*, 2007]. The model domain contains the sub-Arctic North Pacific (including the Sea of Japan and the Sea of Okhotsk) and North Atlantic oceans, the Arctic Ocean, the Canadian Arctic Archipelago (CAA) and the Nordic Seas (Figure 1). Model bathymetry is derived from two sources: ETOPO5 at 5-min resolution for the region south of 64°N and International Bathymetric Chart of the Arctic Ocean (IBCAO [Jakobsson *et al.*, 2000]) at 2.5 km resolution for the region north of 64°N . The ocean model was initialized with climatological, three-dimension-

al temperature and salinity fields (Polar Science Center Hydrographic Climatology; PHC [Steele *et al.*, 2000]) and integrated for 48 years in a spinup mode. During the spinup we initially used daily averaged annual cycle climatological atmospheric forcing derived from 1979–1993 reanalysis from the European Centre for Medium-Range Weather Forecasts (ECMWF) for 27 years. We then performed additional spinup using repeated 1979 ECMWF annual cycle for 6 years and then repeated 1979–1981 interannual fields for the last 15 years of spinup. This approach is especially important to establishing realistic ocean circulation representative of the time period at the beginning of the actual interannual integration. This final run with realistic daily averaged ECMWF interannual forcing starts in 1979 and continues through 2003. Results from this integration (25-years) are used for the analyses in this paper. Yukon (and other Arctic) river runoff is included in the model as a virtual freshwater flux at the river mouth. However, in the Gulf of Alaska the freshwater flux from runoff [Royer, 1981] is introduced only by restoring the surface ocean level (of 5 m) to climatological (PHC) monthly mean temperature and salinity values over a monthly timescale. This restoring acts as a correction term to the explicitly calculated fluxes between the ocean and overlying atmosphere or sea ice and it helps to overcome the lack of data for the many small rivers around the Gulf of Alaska. Additional details on the model including sea ice, river runoff, and restoring have been provided elsewhere [Maslowski *et al.*, 2004].

3. Results

3.1. Model Validation

[7] As already mentioned, Crawford *et al.* [2000] used satellite altimetry data to measure the presence of six anticyclonic eddies in the Alaskan Stream during a 6-year period. Modeled sea surface height anomalies also showed

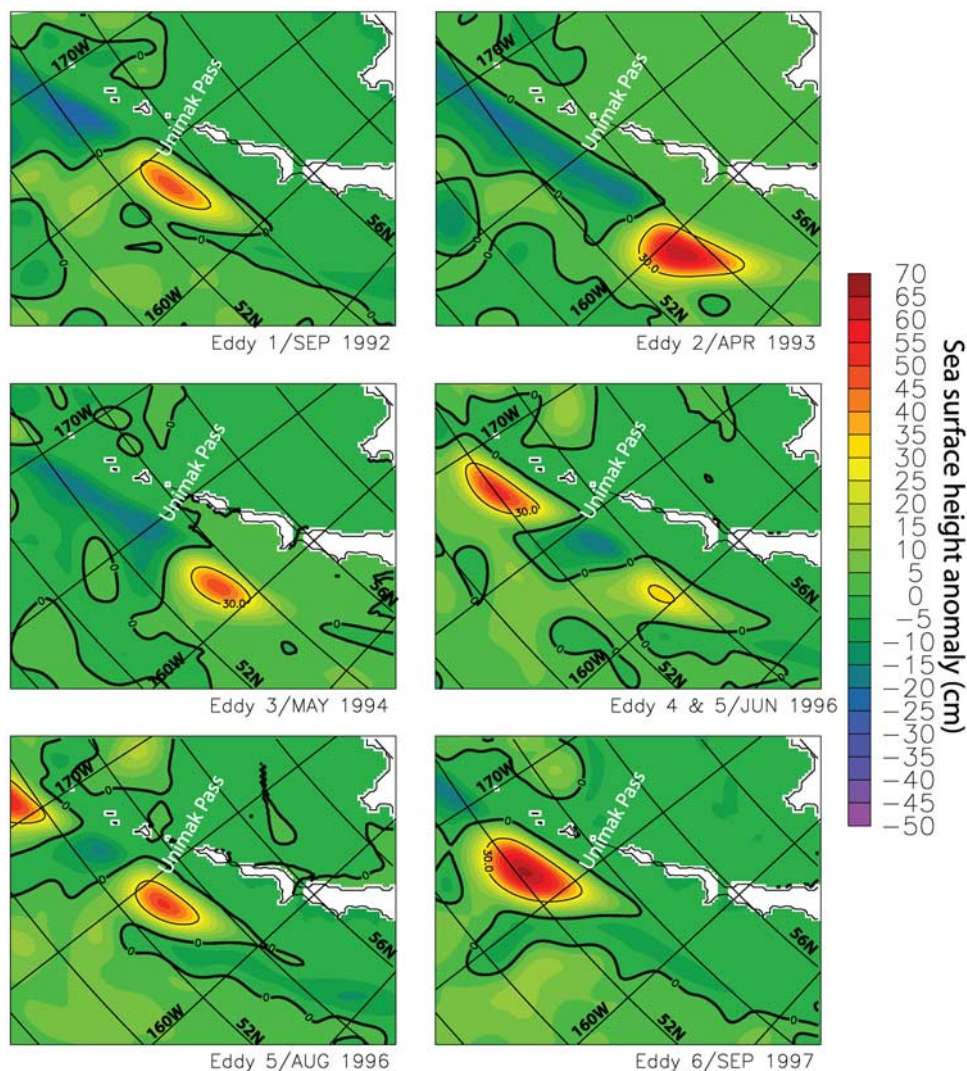


Figure 2. Modeled monthly mean sea surface height anomaly (SSHA) associated with six eddies propagating along the Alaskan Stream during the time period September 1992 through September 1998. Color shading represents the total SSHA (cm).

six eddies propagating westward along the Alaskan Stream during the same period (September 1992 through September 1998; Figure 2). When located just south of Unimak Pass ($\sim 166^{\circ}\text{W}$), the modeled eddies (Eddy 1 through Eddy 6) averaged a maximum sea surface height anomaly (SSHA) and diameter (estimated based on SSHA) of ~ 62 cm and ~ 168 km respectively, both of which are consistent with Crawford *et al.* [2000]. Also, the modeled SSH of eddy 5 increases between June 1996 and August 1996, which is again in agreement with Crawford *et al.* [2000], who state that eddies often increase in height after formation. Lastly, both the modeled eddies (Figure 2), and eddies observed using T/P data were estimated to have life-spans ranging from approximately 1 to 3 years. However, eddies with life-spans of up to 5 years exist [Ladd *et al.*, 2007], which suggests that such estimates could depend on the time period of observations and/or methods of calculation. Note that Crawford *et al.* [2000] found some eddies already existed before and some continued beyond their period of

observations. The six modeled eddies simulated during this time period also appear at different phases of their life cycle. However, it is hard to argue that the observed and modeled eddies are the same features given the limited information about eddies observed by Crawford *et al.* [2000] and known model limitations, such as described next. First, the transient life of modeled eddies is a function of the quality of the prescribed atmospheric forcing, which is definitely less than 100% realistic. In addition, the model representation of volume and property exchanges across many of the Aleutian Island passes is strongly controlled by tides, which are not accounted for in the current model version. In some cases (e.g., Eddy 1, 4, and 5), there is an cyclonic feature associated with the anticyclonic eddy. Eddy 2 will be explored further in the following section, due to its most visible effect on the volume transport across sections AS1 through AS8 (see Figures 3 and 4).

[8] Before continuing discussion of eddies, let us make a note on the transport of Alaskan Stream. The long-term

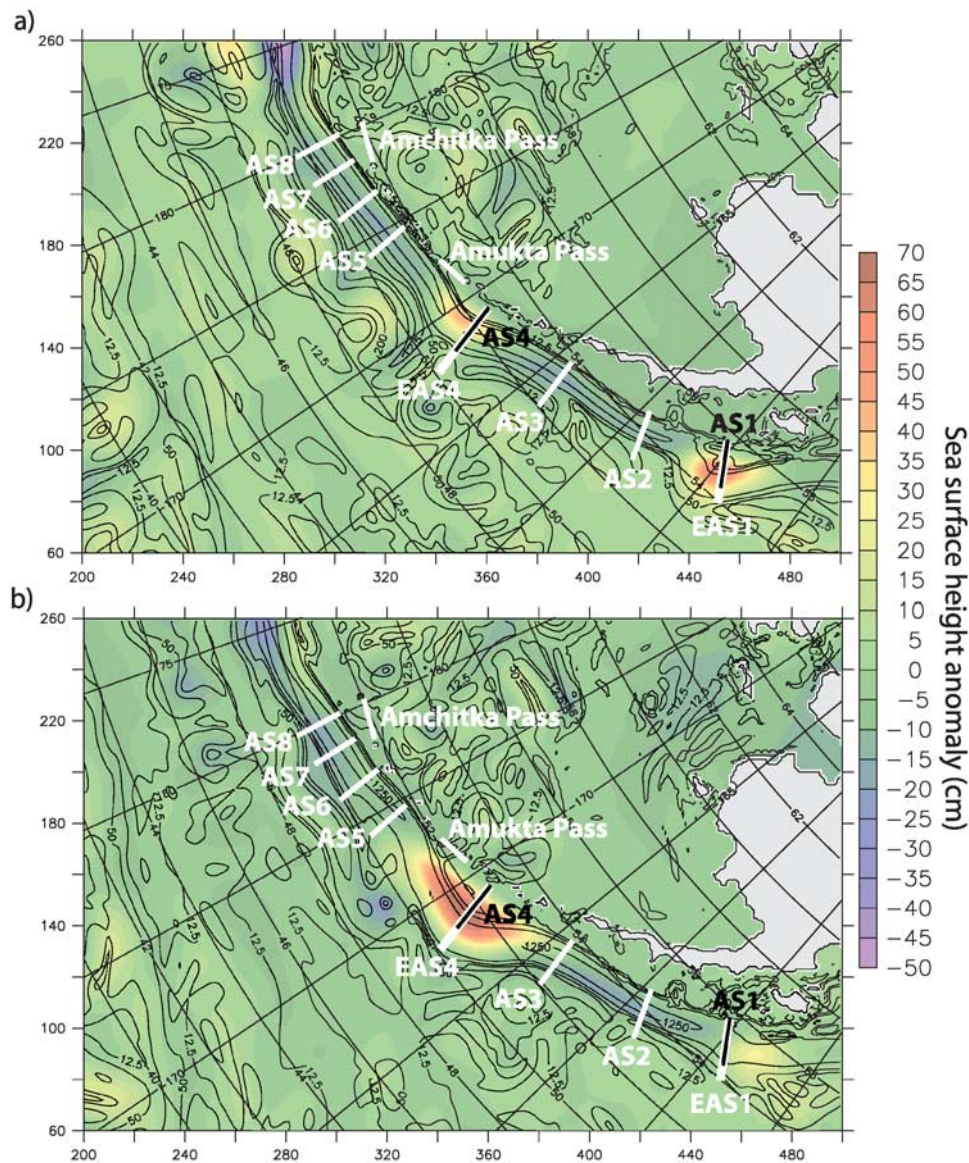


Figure 3. Mean monthly SSHA during (a) January 1993 and (b) December 1993. Color shading represents the SSHA (cm). Contour lines represent total kinetic energy (TKE; $\text{cm}^2 \text{s}^{-2}$) in the upper 477 m. TKE is the velocity²/2. The contour levels shown (12.5, 50, 200, 1250 $\text{cm}^2 \text{s}^{-2}$) correspond to velocities of 5, 10, 20, and 50 cm/s, respectively. The x - and y -axes represent the model grid.

mean modeled volume transport of the Alaskan Stream is estimated between 45 Sv and 56 Sv, intensifying westward [Maslowski et al., 2008] In summary, these are significantly higher than observational estimates of 10–25 Sv [e.g., Reed, 1984; Reed and Stabeno, 1999], which were typically based on geostrophic velocity calculations derived from hydrographic data with assumption of no motion at some depth (e.g., at 1000 m or 1500 m). However, flow estimates of the Alaskan Stream including current meters [Warren and Owens, 1988] or referenced to lower depths [Roden, 1995; Onishi and Ohtani, 1999; Onishi, 2001] yield much higher transports, closer to modeled magnitudes. The baroclinic contribution below and the barotropic above the depth of no-motion are the main correction terms missing and underestimating transport estimates from hydrographic observations of the Alaskan Stream.

3.2. Eddy Effects on the Alaskan Stream During 1993–1995

[9] The examination of eddy 2 will begin southeast of Kodiak Island, because the area to the east of this location is beyond the scope of this report. Eight cross-sections (AS1–AS8) were created along the mean position of the Alaskan Stream, roughly between 155°W and 180°W (locations shown in Figures 3a and 3b). The width of each section was determined from the 26-year mean velocity profile at each location to include all the westward flow associated with the Alaskan Stream. Figures 3a and 3b show the SSHA, as well as the southward displacement of the Alaskan Stream (as seen from total kinetic energy contour lines), as eddy 2 begins to pass both AS1 and AS4 during January 1993 and December 1993, respectively. Propagating along the Alaskan Stream, the lifespan of eddy 2 from

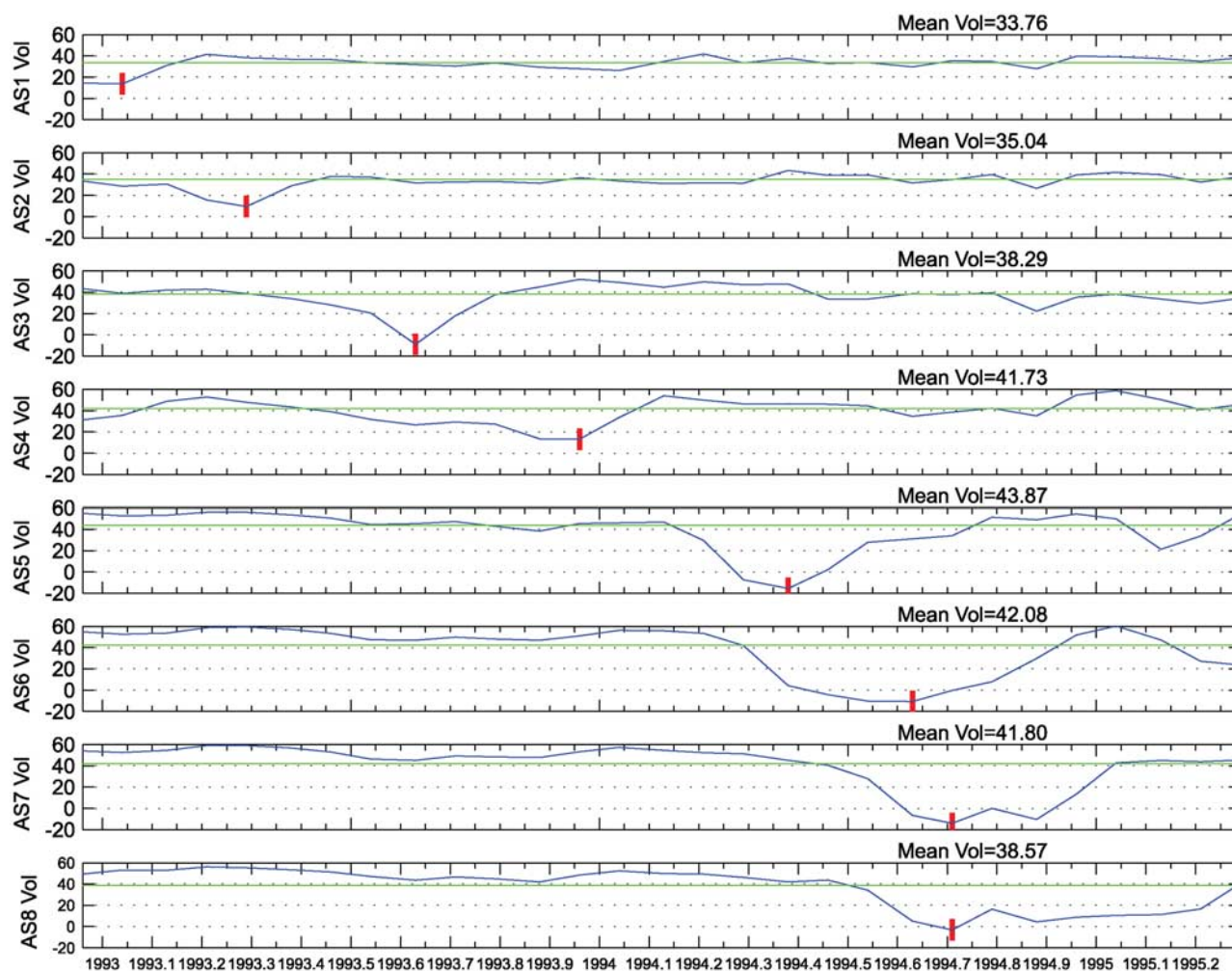


Figure 4. Monthly mean net volume transport over a 29-month time series (January 1993 to May 1995; blue line). The 25-year net mean is represented by the green line. The red tick marks indicate the lowest volume transport for each cross section as the eddy passed through.

AS1 (January 1993) until it dissipated at AS8 (April 1995) was approximately 28 months. Traveling a distance of ~ 1882 km during that period, the modeled phase speed at which eddy 2 propagated westward along the Alaskan Stream was ~ 2.3 km day $^{-1}$. Again, this is in agreement with observations made by Crawford *et al.* [2000] using T/P data, who estimated that the mean speeds of the six eddies witnessed during the September 1992 through September 1998 time period was 2.5 km day $^{-1}$. Figure 4 shows the time series (January 1993 – May 1995) of volume transport at selected cross sections along the Alaskan Stream as eddy 2 propagates from AS1 to AS8. The red vertical line on each graph identifies the lowest volume transport in each cross section as the eddy passes through. From Figures 3a and 3b, as well as Figure 4, it is evident that eddy 2 affected not only the path of the Alaskan Stream at AS1 through AS8, but also affected the volume transport at these locations as well. AS1, with a 25-year mean modeled volume transport of ~ 34 Sv, showed a significant decrease in flow during January 1993, exhibiting a weak westward flow measuring ~ 14 Sv (i.e., $\sim 59\%$ decrease). At AS4, the 25-year mean modeled transport was ~ 42 Sv, and it decreased to ~ 13 Sv

during December 1993 (i.e., $\sim 69\%$ decrease). It is worth noting that the percent and magnitude of transport decrease from the mean at AS4, as compared to AS1, is significantly larger, which is a result of eddy 2 increasing in both diameter and SSHA magnitude as it propagates westward along the Alaskan Stream (see Figures 3a and 3b). The increased size of eddy 2 would result in a greater seaward shift of the Alaskan Stream, reducing the volume transport measured through AS4.

[10] Further examination of Figure 4 also reveals that eddy 2 is moving along the Alaskan Stream at a fairly steady pace until it reaches AS6 (exhibiting a phase speed of ~ 3.35 km day $^{-1}$ from AS1 to AS6), where eddy 2 begins to stall as it nears Amchitka Pass. This is evidenced by the increased amount of time the volume transport remains below the mean at the last three cross sections in Figure 4. The reason for the stalling could be related to ‘eddy shedding’ near Amchitka Pass [Okkonen, 1992] due to the change of sign of relative vorticity which is associated with the northward turn of the bathymetry. At AS6, the modeled mean transport is 42.08 Sv. However, while eddy 2 propagates through this cross section, modeled transport falls

well below the mean from April 1994 till December 1994, during which time it reached a minimum (reversed or eastward) flow of -10.6 Sv. Along AS7, the modeled effects of eddy 2 lasted for 7 months (June 1994–January 1995) and the minimum volume transport was -14 Sv. Lastly, volume transport at AS8 was well below the calculated mean flow (38.57 Sv) from July 1994 until April 1995. The minimum volume transport at AS8 during this period was -3 Sv. The effect of eddy 2 on the Alaskan Stream at cross sections AS6 through AS8 is especially important to the northward flow through Amchitka Pass. Considering AS7 and AS8 are located just upstream and downstream from Amchitka Pass, a reduction, and sometimes reversal, of flow just to the south of the pass will drastically alter the volume transport of water entering the Bering Sea through this important pass. Effects of eddies propagating within the Alaskan Stream on the exchanges through Amukta and Amchitka passes (i.e., the two main passes within the eastern and central Aleutian Chain) are discussed in section 3.6.

3.3. Strength of Alaskan Stream During Southward Shifts

[11] Although it has been shown that the modeled volume transport across AS1–AS8 decreases as eddy 2 propagates through each of the cross sections, the speed of the Alaskan Stream remains relatively strong just south of these sections. Figure 5 shows modeled vertical velocity profiles of sections EAS1 (left) and EAS4 (right), which are basically extended sections AS1 and AS4 (Figure 3), elongated seaward by 74 and 92 km, respectively. The top figures show the 25-year-mean position of the Alaskan Stream at both sections, with the velocity core lying above the continental slope. At both sections, a weak westward flow (in the range of 0 – 5 cm s^{-1}) exists below 2000 m extending all the way to the bottom. The second row of figures shows the velocity during January 1993, when the eddy is at EAS1. An offshore shift in the velocity core of ~ 75 km is seen at EAS1. Further downstream at EAS4 the core is moved offshore by ~ 55 km south from its mean position, but this is due to a different eddy present there in January 1993 (as shown in Figure 3a). On the basis of analysis of surface speeds, which are well over 40 cm s^{-1} at EAS1 during January 1993, it is clear that the flow of the Alaskan Stream during the southward shift is not reduced much, but rather remains relatively intact. Also, the deeper portion of the stream at EAS1 during this period is remarkably strong as well, exhibiting speeds above 5 cm s^{-1} below 1500 m down to the bottom. The modeled volume transport at EAS1 during January 1993 also showed signs of a strong current, reaching a maximum westward flow of ~ 43 Sv, while measuring ~ 25 Sv for the upper 1000 m. This is significant considering that the 25-yr mean modeled westward/net volume transport at AS1 is $\sim 36/34$ Sv and the 25-yr mean westward/net transport at EAS1 is $38/33$ Sv, respectively. It indicates that the Alaskan Stream does not slow down during the southward shift; if anything, it increases in strength.

[12] During December 1993 (third row of Figure 5) the velocity core is transitioning to a more ‘normal’ state at EAS1. At the same time, the core at EAS4 has moved 155 km offshore from its mean position as the eddy crosses this

section. The maximum (monthly mean) surface speed during that time is over 50 cm s^{-1} . Like at EAS1, the core structure at EAS4 at the time of eddy passage is well formed, with the increased westward flow at depth above 5 cm s^{-1} . The respective modeled westward/net volume transport at EAS4 during this time period is $\sim 60/51$ Sv, which is an increase of $\sim 7/14$ Sv (or 13/38%) compared to the 25-yr mean westward/net transport at EAS4 of $53/37$ Sv. More importantly, the respective modeled westward/net (monthly mean) transport across AS4 in December 1993 is only $19/13$ Sv (or $\sim 32/25\%$ of that at EAS4). Finally, the transports at EAS4 during that time are $13/9$ Sv (or $\sim 28/21\%$) higher compared to the 25-year mean westward/net transport at AS4 of $47/42$ Sv, respectively. By August 1994 (bottom row of Figure 5), the velocity cores have stabilized into a position/state that approximates the mean.

3.4. Effect of an Eddy on the Distribution of Salinity

[13] Figure 6 shows monthly mean distributions of velocity every 2 months (left panels) as the 1993 eddy approaches and passes through EAS4. The effect that the eddy has on the horizontal and vertical distribution of salinity is also shown in Figure 6 (right panels). During August 1993, which is 4 months before the eddy reaches EAS4, we see a low salinity core over the shelf with salinity as low as 31.6. The subsurface salinity minimum along the southern Aleutian shelf can be due to the predominately downwelling regime in the region [Batchelder and Powell, 2002; Ware and McFarlane, 1989]. Two months later the low salinity signal is leaked offshore and its surface salinity minimum is aligned with the velocity core that moves ~ 60 km offshore. When the eddy is present at EAS4 (Dec. 1993), the salinity minimum moves more than 200 km to the south. Over the shelf and slope salinities are now over 32, and the isohalines have generally deepened and flattened over much of the cross-section. February 1994 shows a transition back toward the more usual state. Even if the seasonal cycle of salinity is removed, the dynamic effect of the 1993 eddy is clear.

[14] In order to emphasize changes along EAS4 due to the passage of an eddy, Figure 7 shows differences of velocity and salinity over this time period. The top two rows show difference fields for December 1993 minus August 1993 and December 1993 minus October 1993, respectively. Negative salinity differences throughout most of the section represent a lower salinity signal during December 1993 when the eddy is present than 4 and 2 months before. Negative differences are concentrated in the upper 300 m (up to -1.8), with magnitudes at the surface up to -1 . However, close to the slope and over the shelf salinity anomalies are positive. These nearshore positive anomalies are strongest (up to 0.6) in the lower panel (i.e., December 1993 minus February 1994 difference), indicating that the eddy was responsible for bringing relatively salty water up the slope. This result is in qualitative agreement with Okkonen *et al.* [2003] who observed that an anticyclonic eddy (of ~ 200 km diameter) induced upwelling near Kodiak, Alaska based on satellite and hydrographic observations in 1988. Given that higher salinities below the euphotic zone can be used as proxies for increased nutrient concentrations (P. Stabeno, personal communication, 2004), the eddy-induced upwelling along

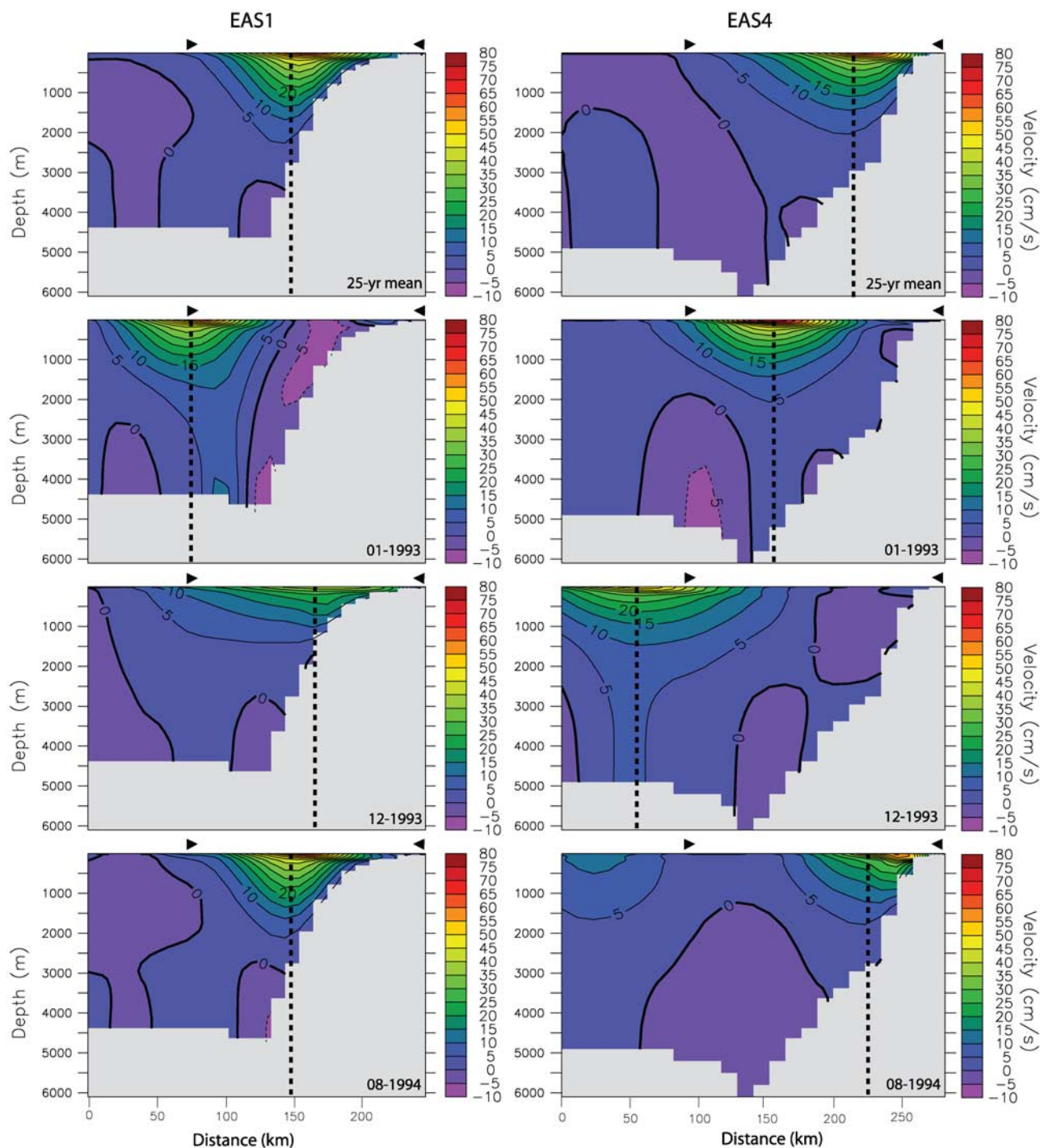


Figure 5. Monthly mean vertical profiles of velocity (cm s^{-1}) for cross sections (left) EAS1, (right) EAS4. Positive velocity is directed westward. Inward-facing triangles above each figure indicate the position of the original sections (AS1 on left; AS4 on right). The black line represents the horizontal position of the velocity core.

the slope might represent a significant influx of nutrients onto the Aleutian shelves.

3.5. The Importance of Eddies in the Alaskan Steam

[15] In attempt to quantify the role of eddies in the transport of the Alaskan Stream, time series of volume transport across AS4 and the extended version EAS4 are

shown for comparison in Figure 8. We see that the long-term 25-year net mean is 41.7 Sv at AS4 with a range of 11–65 Sv. The net mean for EAS4 is somewhat lower (37.1 Sv) due to the inclusion of the region further south with the prevailing eastward component of flow. However, the 25-year mean westward flow associated with the Alaskan Stream is about 12% higher at EAS4 (52.8 Sv) than at

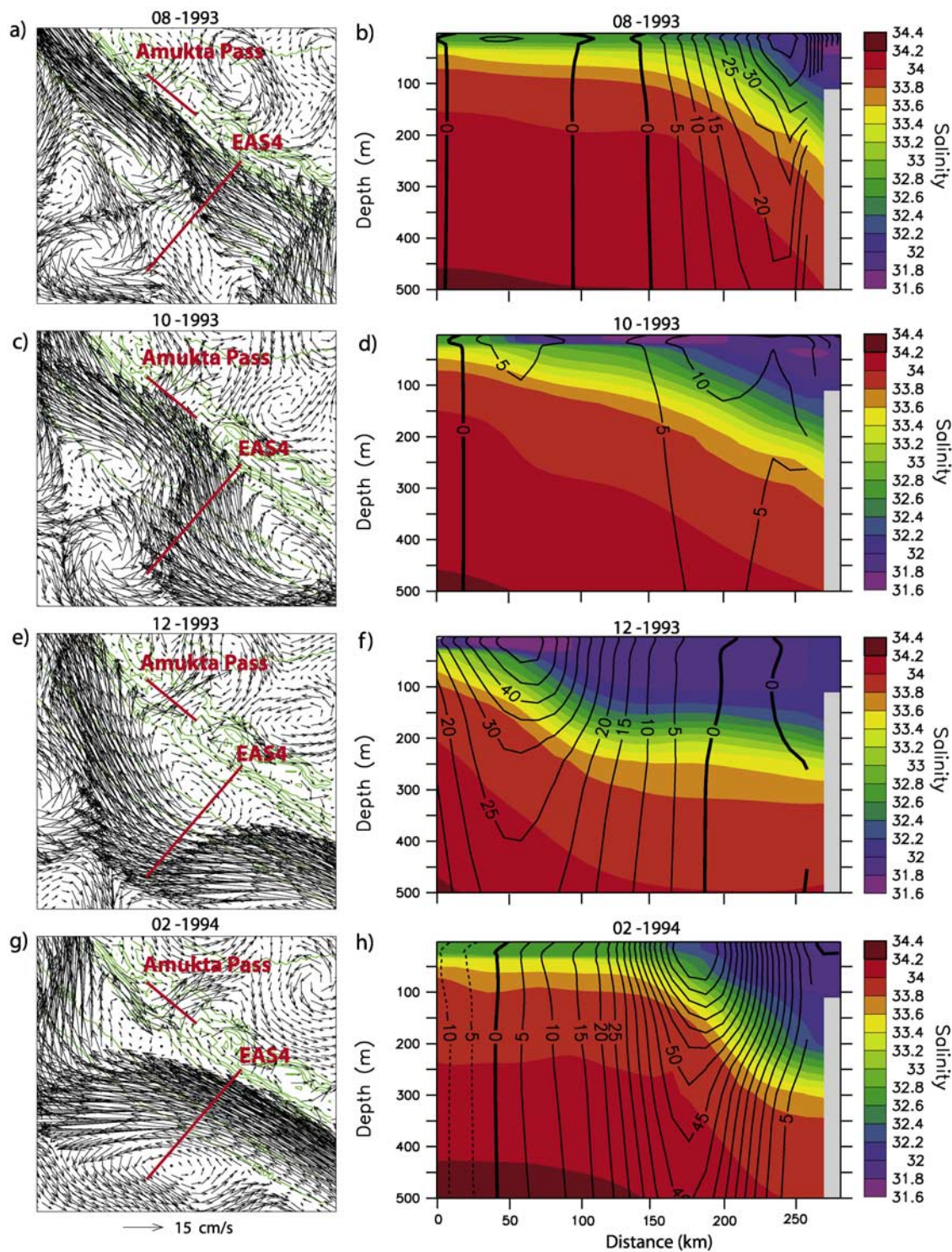


Figure 6. Velocity (left; in upper 500 m) and salinity with overlaid velocity contours (cm s^{-1}) at EAS4 (right) during (a, b) August 1993, (c, d) October 1993, (e, f) December 1993, and (g, h) February 1994. Green lines represent bathymetry (on left).

AS4 (47.3 Sv). The difference in the westward flow between EAS4 and AS4 is shown in Figure 8c. The time series is always positive (i.e., transport at EAS4 is larger or equal to that at AS4), ranging between 0 and 49 Sv, with a number of significant peaks. Almost all of these peaks are associated with eddies crossing the sections (shown as stars

in Figure 8c based on analysis of modeled SSHA fields). A total of 20 eddies, with SSHA greater than 30 cm, crossed the EAS4 line during the 25 years (1979–2003). This is an average of 0.8 per year. For stronger eddies, with SSHA greater than 50 cm, the total is 12 during the same time period for an average of 0.5 per year. These eddies can have

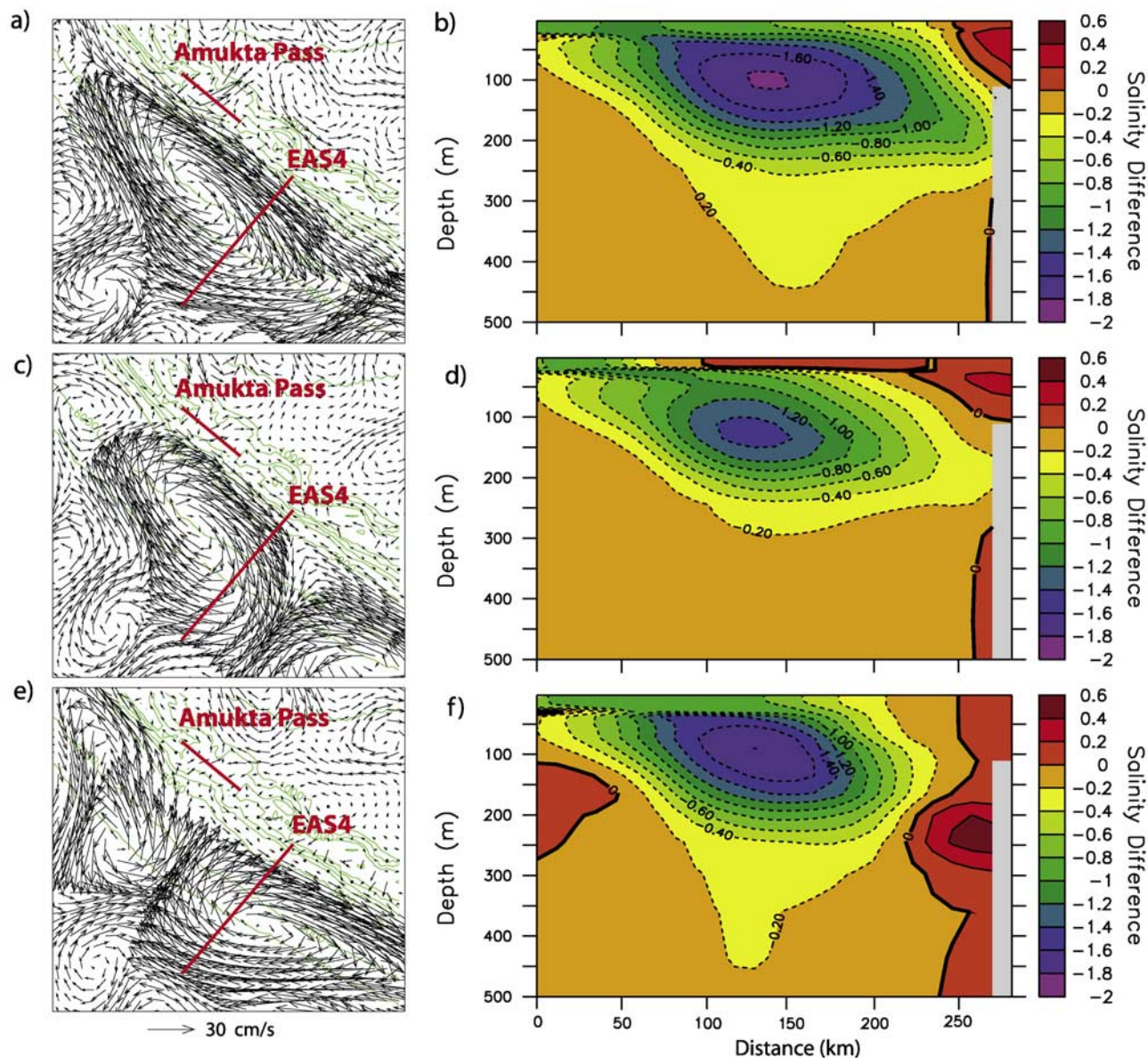


Figure 7. Velocity difference (left; in upper 500 m; cm s^{-1}) and salinity difference at EAS4 (right) for (a, b) December 1993 to August 1993, (c, d) December 1993 to October 1993, and (e, f) December 1993 to February 1994. Green lines represent bathymetry (on left).

a large impact on the flow, stratification, and property exchange across the slope as they propagate along the Alaskan Stream. Several strong eddies (1979, 1984, 1987, 1990, 1993, 1997, 2002, and 2003) create a difference upwards of 20 Sv between the sections.

3.6. The Effect of Eddies on Exchanges With the Bering Sea

[16] In this section we discuss effect of eddies propagating within the Alaskan Stream on exchanges through Amukta and Amchitka Pass (i.e., the two main passes of the Aleutian Island Chain). In addition to volume fluxes we calculated volume flux anomalies, by subtracting the 25-year mean annual cycle of volume flux (listed in Table 1) from an actual volume flux for a given month (e.g., the long-term mean January value was subtracted from the

January 1979 value to obtain the anomaly during Jan. 1979). Heat flux was calculated as a sum of products of volume flux and temperature difference above the reference temperature of -0.1°C , over a vertical section. Similarly, freshwater flux was calculated as a sum of products of volume flux and salinity difference below the reference salinity of 33.8 normalized against the reference salinity.

[17] Time series of volume flux anomalies through Amukta and Amchitka Pass are shown in Figure 9. The stars indicate months when the center of a propagating eddy is nearest Amukta (Figure 9a) or Amchitka (Figure 9b) Pass. Red stars represent “strong” eddies with sea surface height anomalies (SSHA) of >50 cm, while blue stars indicate “weak” eddies with $30 \text{ cm} < \text{SSHA} < 50$ cm.

[18] Effect of the previously discussed eddy (shown in Figures 6–7) on the flow through Amukta Pass is summa-

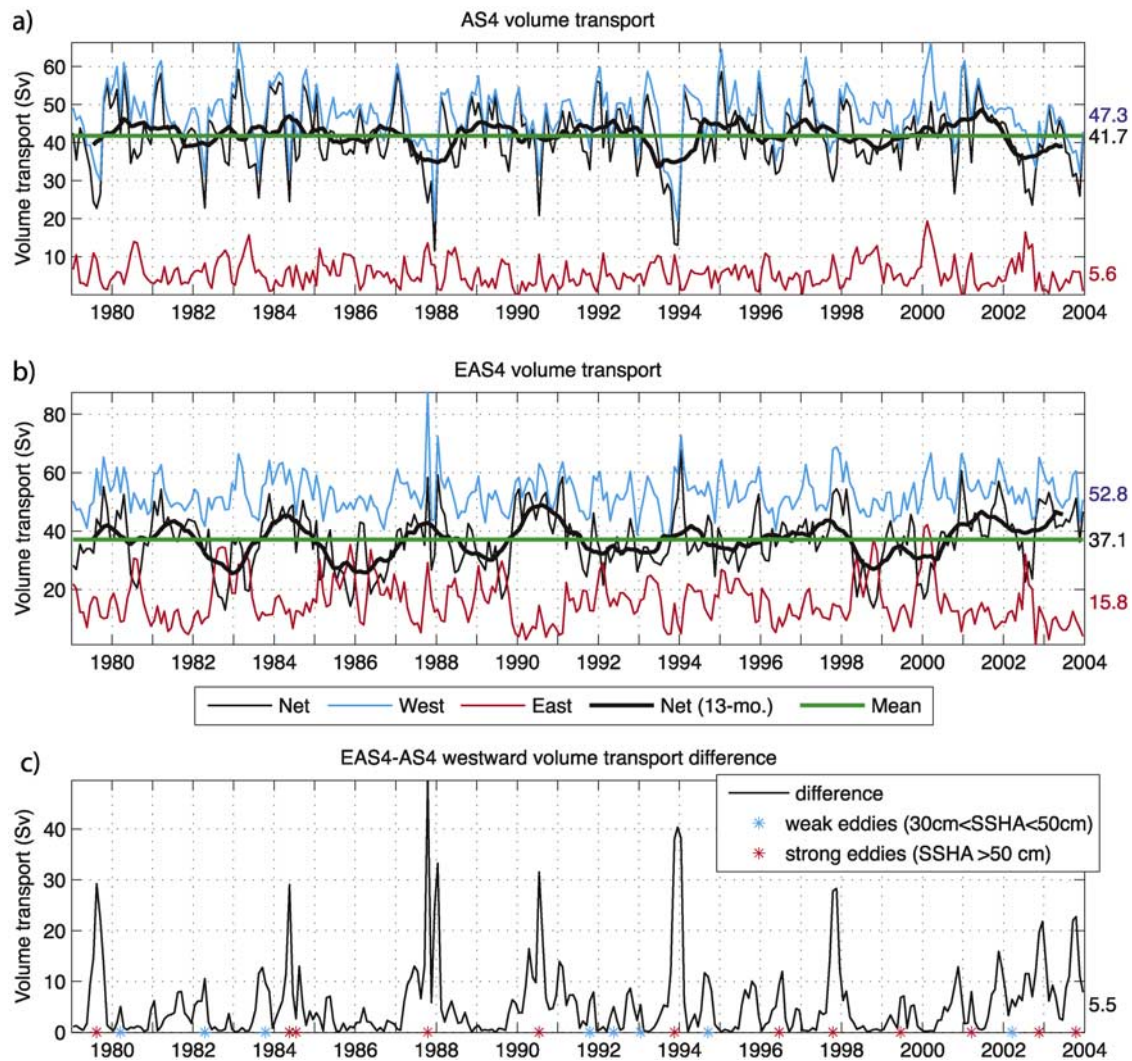


Figure 8. Monthly mean time series of volume transport across (a) AS4, (b) EAS4, and the westward volume transport difference across (c) EAS4 – AS4. The presence of weak eddies ($30 \text{ cm} < \text{SSHA} < 50 \text{ cm}$) is marked with a blue star, while the presence of strong eddies ($\text{SSHA} > 50 \text{ cm}$) is marked with a red star. The mean difference of 5.5 Sv is shown on the right side of the bottom panel.

alized in Table 2, which shows statistics on the volume, salt and heat flux occurring during its passage (September 1993 – May 1994). Mean (9-month) volume flux/anomaly during this time period was 2.43 Sv/0.78 Sv, which is 53% greater/7% less than the 25-year all time mean of 1.59 Sv/0.84 Sv, respectively (see Tables 1 and 2). Note that the mean modeled transport at Amukta Pass is less than the recent estimate by *Stabeno et al.* [2005] of ~ 4 Sv, based on 24 months of current data from four moorings in the early 2000s. Several factors can help explain such a difference and they include: the absence of tides in the model, the model representation of bottom bathymetry in the pass, spatial distribution of current meters in the section, different period of observations versus model simulation. Also, previous estimates from hydrographic surveys [*Reed and Stabeno*, 1997] were approximately five times as small as the transport from the moorings. However, most importantly *Stabeno et al.* [2005] have found in agreement with this study that at monthly and longer timescales the volume

transport through Amukta Pass was related to the position and strength of the Alaskan Stream.

[19] Similarly, salt and heat fluxes through Amukta Pass were above average during the passage of the eddy with 9-month means of 79 million kg/s and 58 TW compared to the respective 25-year all time means of 52 million kg/s and 39 TW. Note that comparison against the 25-year September–May means yields only slightly different relative changes. This eddy shown to be centered south of Amukta Pass during February 1994 (Figure 6g) reaches a downstream location near Amchitka Pass in January 1995, as indicated by the red star in Figure 9b. The eddy is associated with greatly increased northward volume and property flow (up to 5 Sv, 165 million kg/s, and 100 TW above the mean) through Amchitka Pass for several months.

[20] Maximum anomalies at Amukta Pass during 1979–2003 are simulated in early 1998, when monthly mean volume, salt, and heat flux anomalies reach 2.5 Sv, 82 million kg/s, and 60 TW, respectively. At Amchitka Pass

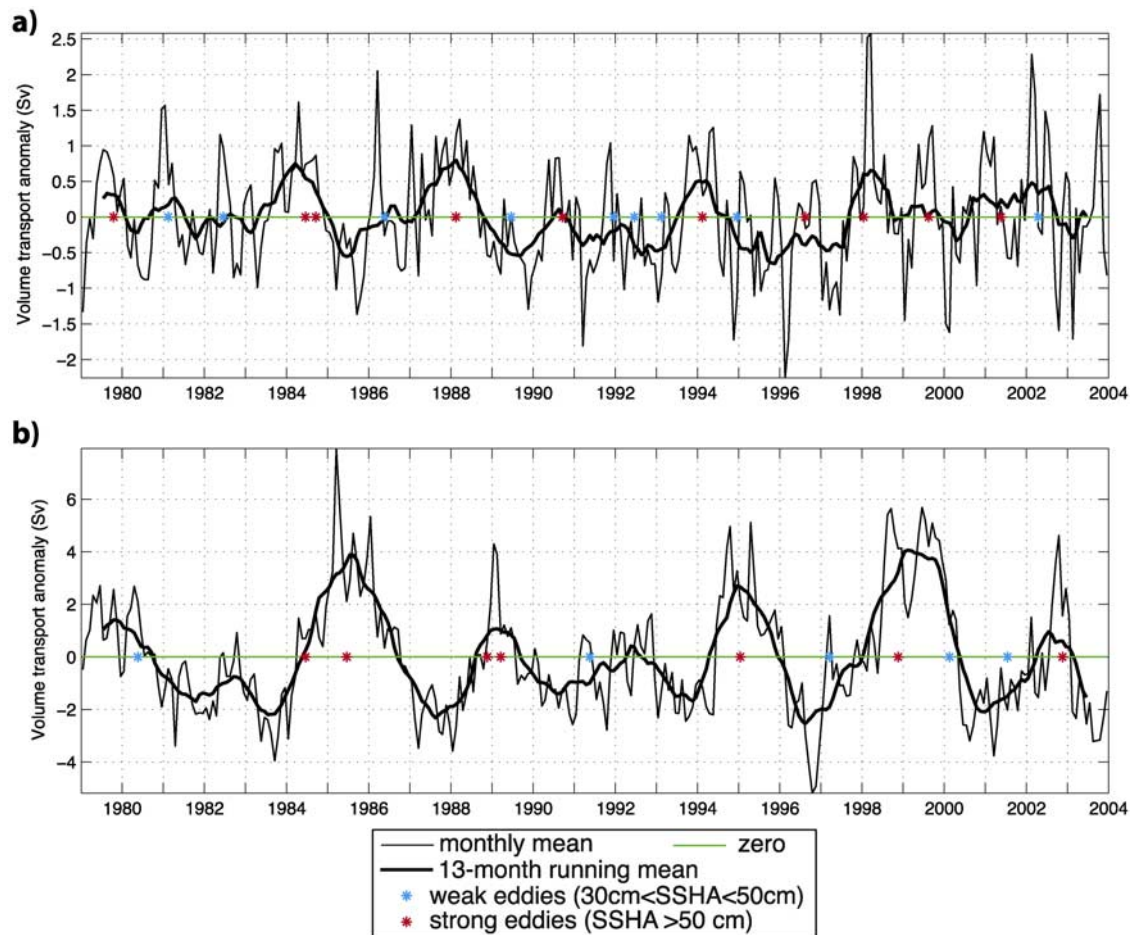


Figure 9. Monthly mean time series of volume transport anomaly across (a) Amukta Pass section and (b) Amchitka Pass section. The thick black line represents a 13-month running mean. The presence of weak eddies ($30 \text{ cm} < \text{SSHA} < 50 \text{ cm}$) is marked with a blue star, while the presence of strong eddies ($\text{SSHA} > 50 \text{ cm}$) is marked with a red star.

the most extreme effect of a passing eddy occurs in 1985 with respective anomalies reaching up to 8 Sv, 265 million kg/s, and 150 TW. The all time 25-year modeled volume, heat and salt flux means for this pass are 1.89 Sv, 62 million kg/s and 45 TW (Table 1), respectively. Only 12 eddies are identified near Amchitka Pass versus the 20 that were identified near Amukta Pass. High monthly mean anomalies of volume and property transport through both passes tend to be associated with the presence of strong eddies. Because heat flux and salt flux are highly correlated with volume flux (both correlation coefficients are greater than 0.98), time series of these properties are not shown as they have very similar variabilities to those shown in Figure 9.

4. Discussion

[21] From the results of our model, and from observational results by *Reed and Stabeno* [1989, 1999] and *Crawford et al.* [2000], we conclude that the Alaskan Stream remains relatively intact during the periods of southward shifts. Also, we believe that the formation and propagation of eddies along the Alaskan Stream is the main cause of these deviations in the westward flow. Any stationary attempt to monitor the flow of the Alaskan

Stream (e.g., moored ADCP) could interpret an eddy as a decrease or disappearance of the current. However, measurements made to the south of the mean position of the current will likely capture the velocity core. For example, the CTD data collected by *Reed and Stabeno* [1999] suggest a significant reduction in the volume transport of the Alaskan Stream located near 170°W , while satellite altimetry data revealed the presence of a strong anticyclonic eddy centered near 167°W during May 1997. A comparison of model results between AS4 and EAS4 (Figure 8), both located around 168°W , suggests the passage of a strong eddy around the same time, which accounted for ~ 28 Sv difference in westward transports between the extended (EAS4) and shorter (AS4) sections. Similarly, the observations of ‘nearly absent’ westward flow south-west of Kodiak Island (i.e., near AS1) during spring of 1986 and 1987 by *Reed and Stabeno* [1989] could be related to the passage of one of the strongest eddies during the 1979–2004 period. Assuming a similar propagation speed as for the 1993 eddy, this eddy would have arrived at EAS4 in late 1987 (Figure 8) where it accounted for close to 50 Sv difference in westward transports between EAS4 and AS4. The importance of these deviations in the path of the Alaskan Stream and the subsequent impact on northward

Table 1. 25-Year Mean Volume Transport (Sv) Heat Flux (TW), and Salt Flux (Million kg/s) for Each Month (and the Overall 25-Year Mean) for Amukta and Amchitka Passes^a

Month	Amukta Pass			Amchitka Pass		
	Vol. Trans.	Heat Flux	Salt Flux	Vol. Trans.	Heat Flux	Salt Flux
1	2.02 (0.85)	47.65 (20.38)	65.57 (27.54)	2.39 (2.27)	51.89 (46.17)	78.94 (76.00)
2	2.26 (1.08)	50.71 (24.44)	73.29 (35.03)	2.87 (1.81)	60.06 (35.94)	94.95 (60.85)
3	1.85 (1.15)	41.52 (26.70)	60.18 (37.51)	2.64 (2.39)	54.99 (46.07)	87.36 (80.43)
4	1.47 (0.65)	32.92 (15.18)	47.67 (21.36)	2.39 (2.48)	51.51 (49.34)	79.08 (83.58)
5	1.35 (0.67)	31.98 (15.52)	43.97 (21.95)	1.39 (1.86)	33.75 (37.88)	45.45 (62.76)
6	1.48 (0.62)	37.47 (15.78)	47.96 (20.27)	0.94 (1.90)	27.28 (39.80)	30.24 (64.05)
7	1.38 (0.63)	36.72 (16.82)	44.72 (20.66)	1.30 (1.96)	37.05 (42.24)	42.24 (65.99)
8	1.20 (0.61)	32.67 (16.35)	38.83 (20.00)	1.55 (2.35)	43.68 (52.46)	50.87 (78.87)
9	1.20 (0.69)	33.09 (18.92)	38.89 (22.65)	1.84 (2.76)	50.32 (62.38)	60.45 (92.69)
10	1.44 (0.80)	38.58 (21.28)	46.79 (26.26)	1.89 (2.80)	50.82 (64.61)	62.31 (93.43)
11	1.53 (0.76)	39.04 (19.28)	49.69 (24.91)	1.49 (2.17)	37.08 (48.92)	49.09 (72.22)
12	1.90 (0.65)	46.57 (16.71)	61.65 (21.10)	1.95 (2.20)	43.51 (46.36)	64.61 (73.47)
25-yr mean	1.59 (0.84)	39.08 (19.88)	51.60 (27.20)	1.89 (2.30)	45.16 (48.44)	62.13 (77.04)

^aThe standard deviation is shown below each mean in parenthesis. The reference temperature for heat flux calculations is -0.1°C .

flow across the shelf and through the Aleutian Island passes is likely to have a significant effect on the Bering Sea water properties. As an example, we have shown that the presence of an eddy removes low salinity water of the upper ocean near a pass (Amukta Pass) away (i.e., south) from the shelf, but also increases upwelling of high-salinity water along the slope and over the shelf. A change in the frequency and/or strength of these processes could affect the productivity of the surrounding ecosystem.

[22] In Table 3 a statistical summary of volume and property fluxes across EAS4 during 1979–2003 is presented, including mean, annual cycle, and extreme values of these fluxes and time of their occurrence. First, it is important to note that at the southern end of this section an extension of the opposite flow to the Alaskan Stream is captured [Thompson, 1972; Warren and Owens, 1988; Onishi and Ohtani, 1999; Onishi, 2001; Chen and Firing, 2006]. This so-called “eastward jet” [Warren and Owens, 1988] is a well organized current west of $\sim 170^{\circ}\text{W}$. It is located just south of the Alaska Stream and can be interpreted as the northern branch of the North Pacific Current. It is a separate circulation feature from the Alaskan Stream and is not associated with the stream’s potential reversals due to eddy propagation. Hence the westward, rather than net, transports shown in Table 3 might be more representative of the strength of the Alaskan Stream.

[23] The modeled 1979–2003 mean annual cycle (Table 3) shows maximum westward/net volume transport at EAS4 of 58/42 Sv (both) in January and the minimum of 50/33 Sv in August/July, which amount to a range from +9/14% to $-6/11\%$ of the 25-year mean at 53/37 Sv, respectively. Mean seasonal fluxes of other properties, including heat, freshwater and salt, experience similar or even smaller ranges compared to that of volume with some alterations to their timing due to different annual cycles of temperature and salinity. However, much higher ranges of interannual variability of volume and property fluxes are modeled. During 1979–2003, the maximum net monthly mean volume transport at EAS4 was 68 Sv in January 1994 (up by +83% compared to the mean) and the minimum was 13 Sv in October 1992 (down by 65%). Respectively, the maximum westward monthly mean volume transport at EAS4 was 87 Sv in October 1987 (up by +65%) and the minimum was 37 Sv in September 1993 (down by 30%). Heat,

freshwater and salt fluxes also have significantly larger interannual variability compared to the ranges due to respective annual cycles.

[24] Further analysis of results in Table 3 and in Figure 8 suggests that the mean net flow approximately represents the state of minimum westward and eastward fluxes, i.e., without eddies. The maximum westward fluxes are associated with strong eddies. The relative increase in eddy frequency since the late 1990s [Ladd *et al.*, 2007] could have important effects on the circulation and ecosystem dynamics and could contribute to the overall regime shift in the Gulf of Alaska [Bond *et al.*, 2003].

[25] Investigation of eddy effects on exchanges between the Gulf of Alaska and the Bering Sea reveals significant increases in net northward fluxes as an eddy moves along a pass within the Aleutian Islands. Analysis of modeled time series through the two main passes in the eastern and central Aleutian Archipelago, i.e., Amukta Pass and Amchitka Pass, implies very strong effect of passing eddies within the Alaskan Stream on the flow through each pass into the Bering Sea. More importantly, the high correlation (>0.98) of volume flux against salt and heat fluxes at both passes implies the dominant role of velocity/volume flux variability on the property fluxes. Eddy 2 (analyzed earlier) increases volume, salt and heat fluxes by roughly 50%, compared to the 25-year means. According to Figure 9, this was one of the 10 strong eddies (i.e., SSHA > 50 cm) simulated during 1979–2003. The largest effect of the modeled eddy on fluxes through Amukta Pass occurred in 1998 (Figure 9), when volume, salt, and heat fluxes compared to the 25-year means (Table 1) increased by 277%, 258%, and 271%, respectively. At Amchitka Pass, there were 7 strong eddies with the largest effect of a modeled

Table 2. Volume and Property Transport Statistics for September 1993 to May 1994 Across Amukta Pass Section During the Passage of an Eddy^a

	9-Month Mean	Mean of Anomalies
Volume flux	2.43	0.78
Salt flux	79.37	25.80
Heat flux	57.66	17.71

^aAnomalies are calculated from the 25-year (1979–2003) time series. Units of volume/heat/salt flux are Sv/terawatts (TW)/ 10^6 kg s $^{-1}$, respectively.

Table 3. Volume and Property Transport Statistics Based on Time Series of Monthly Averages at EAS4 for 1979–2003^a

	Volume Transport, Sv			Heat Flux, TW			Freshwater Flux, mSv			Salt Flux, 10 ⁶ kg/s		
	Net	West	East	Net	West	East	Net	West	East	Net	West	East
A.C. mean	37	53	16	670	835	164	279	293	13	1255	1798	542
Min/mo.	33/Jul	50/Aug	14/Dec	640/Jul	816/May	141/Dec	260/May	273/May	10/Apr	1108/Jul	1686/Aug	473/Dec
Max/mo.	42/Jan	58/Jan	18/Jul	705/Oct	862/Oct	195/Jul	301/Oct	316/Nov	16/Nov	1411/Jan	1970/Jan	605/Jul
Monthly min.	13	37	1	371	659	17	201	208	0	430	1254	41
% of mean	35	70	8	55	79	11	72	71	0	34	70	8
Mo./Yr.	10/1982	9/1993	10/2002	10/1998	12/1992	10/2002	4/2003	4/2003	4/1990	10/1982	9/1993	10/2002
Monthly max.	68	87	42	969	1158	463	406	409	55	2313	2989	1452
% of mean	183	165	268	145	139	282	146	140	416	184	166	268
Mo./Yr.	1/1994	10/1987	2/2000	1/1994	10/1987	10/1998	10/2003	10/2003	10/1987	1/1994	10/1987	2/2000

^aThe top row shows statistics (mean, minimum and month, maximum and month) of the respective annual cycles (A. C.). The middle and bottom rows are the respective all time minima and maxima, percentage of change relative to the mean, and month and year of occurrence based on the entire record. Values are rounded to the nearest integer. Units of heat/freshwater are terawatts (TW)/miliSverdrups (mSv; 1 mSv = 10³ m³ s⁻¹ = 0.001 Sv), respectively.

eddy in 1985, when the respective fluxes increased by 523%, 527%, and 433%. Theoretically, an eddy-induced increase in flow through the Aleutian Island passes (including heat fluxes) could be a contributor to the recent warming in the Arctic Ocean, as more warm water entering the Bering Sea can ultimately affect the water and air properties transported northward through the Bering Strait during spring and summer [Clement *et al.*, 2005; Stroeve and Maslowski, 2007; Maslowski *et al.*, 2007].

[26] **Acknowledgments.** We thank the National Science Foundation, the U.S. Department of Energy, and the National Oceanic and Atmospheric Administration (W.M. and J.C.K.) and the Office of Naval Research (R.R.) for support of this research. Computer resources were provided by the Arctic Region Supercomputing Center (ARSC) through the U.S. Department of Defense High Performance Computer Modernization Program (HPCMP).

References

- Batchelder, H. P., and T. M. Powell (2002), Physical and biological conditions and processes in the northeast Pacific Ocean, *Prog. Oceanogr.*, *53*, 105–114.
- Bond, N. A., J. E. Overland, M. Spillane, and P. Stabeno (2003), Recent shifts in the state of the North Pacific, *Geophys. Res. Lett.*, *30*(23), 2183, doi:10.1029/2003GL018597.
- Chen, S., and E. Firing (2006), Currents in the Aleutian Basin and subarctic North Pacific near the dateline in summer 1993, *J. Geophys. Res.*, *111*, C03001, doi:10.1029/2005JC003064.
- Clement, J. L., W. Maslowski, L. Cooper, J. Grebeier, and W. Walczowski (2005), Ocean circulation and exchanges through the northern Bering Sea - 1979–2001 model results, *Deep Sea Res., Part II*, *52*, 3509–3540, doi:10.1016/j.dsr2.2005.09.010.
- Crawford, W. R. (2005), Heat and fresh water transport by eddies into the Gulf of Alaska. Topical Studies in Oceanography: Haida Eddies: Mesoscale transport in the Northeast Pacific, *Deep Sea Res., Part II*, *52*(7–8), 893–908.
- Crawford, W. R., J. Y. Cherniawski, and M. G. G. Forman (2000), Multi-year meanders and eddies in the Alaskan Stream as observed by TOPEX/Poseidon altimeter, *Geophys. Res. Lett.*, *27*(7), 1025–1028.
- Cummins, P. F., and L. A. Mysak (1988), A quasi-geostrophic circulation model of the Northeast Pacific. part I: A preliminary numerical experiment, *J. Phys. Oceanogr.*, *18*, 1261–1286.
- Jakobsson, M., N. Cherkis, J. Woodward, R. Macnab, and B. Coakley (2000), New grid of Arctic bathymetry aids scientists and mapmakers, *Eos Trans. AGU*, *81*(9), 89.
- Ladd, C., C. W. Mordy, N. B. Kachel, and P. J. Stabeno (2007), Northern Gulf of Alaska eddies and associated anomalies, *Deep Sea Res., Part I*, *54*, 487–509, doi:10.1016/j.dsr.2007.01.006.
- Maslowski, W., D. Marble, W. Walczowski, U. Schauer, J. L. Clement, and A. J. Semtner (2004), On climatological mass, heat, and salt transports through the Barents Sea and Fram Strait from a pan-Arctic coupled ice-ocean model simulation, *J. Geophys. Res.*, *109*, C03032, doi:10.1029/2001JC001039.
- Maslowski, W., J. L. Clement, and J. Jakacki (2007), Towards prediction of Arctic environmental change, *Comput. Sci. Eng.*, *9*(6), 29–34.
- Meyers, S. D., and S. Basu (1999), Eddies in the eastern Gulf of Alaska from TOPEX/POSEIDON altimetry, *J. Geophys. Res.*, *104*(C6), 13,333–13,344.
- Musgrave, D. L., T. J. Weingartner, and T. C. Royer (1992), Circulation and hydrography in the northwestern Gulf of Alaska, *Deep Sea Res., Part I or Part II*, *39*(9A), 1499–1519.
- Okkonen, S. R. (1992), The shedding of an anticyclonic eddy from the Alaskan Stream as observed by the GEOSAT Altimeter, *Geophys. Res. Lett.*, *12*, 2397–2400.
- Okkonen, S. R. (1996), The influence of an Alaskan Stream eddy on flow through Amchitka Pass, *J. Geophys. Res.*, *101*(C4), 8839–8851.
- Okkonen, S. R., T. J. Weingartner, S. L. Danielson, D. L. Musgrave, and G. M. Schmidt (2003), Satellite and hydrographic observations of eddy-induced shelf-slope exchange in the northwestern Gulf of Alaska, *J. Geophys. Res.*, *108*(C2), 3033, doi:10.1029/2002JC001342.
- Onishi, H. (2001), Spatial and temporal variability in a vertical section across the Alaskan Stream and Subarctic Current, *J. Oceanogr.*, *57*, 79–91.
- Onishi, H., and K. Ohtani (1999), On seasonal and year to year variation in flow of the Alaskan Stream in the central North Pacific, *J. Oceanogr.*, *55*, 597–608.
- Reed, R. K. (1984), Flow of the Alaskan Stream and its variations, *Deep Sea Res., Part I or Part II*, *31*, 369–386.
- Reed, R. K. (1990), A year-long observation of water exchange between the North Pacific and the Bering Sea, *Limnol. Oceanogr.*, *35*(7), 1604–1609.
- Reed, R. K., and P. J. Stabeno (1989), Recent observations of variability in the path and vertical structure of the Alaskan Stream, *J. Phys. Oceanogr.*, *19*, 1634–1642.
- Reed, R. K., and P. J. Stabeno (1997), Long-term measurements of flow near the Aleutian Islands, *J. Mar. Res.*, *55*, 565–575.
- Reed, R. K., and P. J. Stabeno (1999), A recent full-depth survey of the Alaskan Stream, *J. Oceanogr.*, *55*, 79–85.
- Roden, G. I. (1995), Aleutian Basin of the Bering Sea: Thermohaline, oxygen, nutrient, and current structure in July 1993, *J. Geophys. Res.*, *100*, 13,539–13,554.
- Royer, T. C. (1981), Baroclinic transport in the Gulf of Alaska. part II: A fresh water driven Coastal Current, *J. Mar. Res.*, *39*, 251–266.
- Stabeno, P. J., and R. K. Reed (1992), A major circulation anomaly in the western Bering Sea, *Geophys. Res. Lett.*, *19*, 1671–1674.
- Stabeno, P. J., D. G. Kachel, N. B. Kachel, and M. E. Sullivan (2005), Observations from moorings in the Aleutian Passes: Temperature, salinity and transport, *Fish. Oceanogr.*, *14*(Suppl. 1), 39–54.
- Steele, M., R. Morley, and W. Ermold (2000), PHC: A global ocean hydrography with a high quality Arctic Ocean, *J. Clim.*, *14*(9), 2079–2087.
- Stroeve, J., and W. Maslowski (2007), Arctic sea ice variability during the last half century, in *Climate Variability and Extremes During the Past 100 Years*, edited by S. Brönnimann *et al.*, *Adv. Global Change Res.*, *33*, Springer, New York.
- Thompson, R. E. (1972), On the Alaskan Stream, *J. Phys. Oceanogr.*, *2*, 363–371.
- Ware, D. M., and G. A. McFarlane (1989), Fisheries production domains in the northeast Pacific Ocean, in *Effects of Ocean Variability on Recruitment and an Evaluation of Parameters Used in Stock Assessment Models*, edited by R. J. Beamish and G. A. McFarlane, *Can. Spec. Publ. Fish. Aquat. Sci.*, *108*, pp. 359–379.
- Warren, B. A., and W. B. Owens (1988), Deep currents in the central Subarctic Pacific Ocean, *J. Phys. Oceanogr.*, *18*, 529–551.

J. C. Kinney, W. Maslowski, and R. Roman, Department of Oceanography, Naval Postgraduate School, 833 Dyer Road, Monterey, CA 93943, USA. (maslowsk@nps.edu)